Nanoscale Research Letters

NANO EXPRESS Open Access

Excellent Light Confinement of Hemiellipsoid- and Inverted Hemiellipsoid-Modified Semiconductor Nanowire Arrays

Xinyu Chen[1†], Jiang Wang[1†], Pengfei Shao[1], Qiming Liu[1], Dequan Liu[1], Qiang Chen[2], Yali Li[1*], Junshuai Li[1*] and Deyan He[1]

Abstract

In this paper, we introduce hemiellipsoid- and inverted hemiellipsoid-modified semiconductor nanowire (NW) optical structures, and present a systematic investigation on light management of the corresponding arrays based on GaAs. It is found that the modification makes well utilization of light scattering and antireflection, thus leading to excellent light confinement with limited effective thickness. For example, 90% and 95% of the incident photons with the energy larger than the bandgap energy can be trapped by the inverted hemiellipsoid-modified NW arrays with the effective thicknesses of only ~ 180 and 270 nm, respectively. Moreover, excellent light confinement can be achieved in a broad range of the modification height. Compared to the corresponding array without top modification, spatial distribution of the photo-generated carriers is expanded, facilitating carrier collection especially for the planar *pn* junction configuration. Further investigation indicates that these composite nanostructures possess excellent omnidirectional light confinement, which is expected for advanced solar absorbers.

Keywords: Optical properties, Photovoltaic, GaAs, Solar cells, Physical optics

Background

Solar electricity based on the photovoltaic (PV) effect has made a remarkable progress in the past decades,and is gradually changing the global energy structure [1–10]. To meet the continuously increasing demand of PV electricity, large-scale deployment of PV modules is urgent, and meanwhile restricted by the relatively high price, which is mainly related to high material costs of the market-dominated PV products based on crystalline silicon wafers [11–20]. Although thin film-based PV devices have the huge potential for material cost reduction, poor light absorption due to the limited optical thickness is a big concern and needs to be addressed by introducing light management structures, such as antireflection coatings and/or substrate texturing, which would result in the extra cost [21–27].

Different from the traditional planar structures, nanostructured semiconductor solar absorbers possess superior properties in light management and photo-generated carrier collection and thus exhibit huge potential in application of high performance-to-cost optoelectronic devices including solar cells and photodetectors [28–36]. Thanks to the extensive efforts dedicated by the related researchers, various semiconductor nanostructures such as nanowire (NW) [37–45], nanocone [46–50], nanopit [51–53], and nanohemisphere [54, 55] arrays have been introduced and investigated from both theoretical and experimental aspects. Effects of light management modes including modification of spatial refractive index for antireflection, leaky mode, guided longitudinal resonance, light scattering, and surface plasmon resonance on light trapping have been understood and emphasized with different weights for different nanostructures [56–61]. However, each individual light management mode cannot fulfill efficient light confinement in a broad spectral range, especially for solar cell applications. Accordingly,

* Correspondence: liyli@lzu.edu.cn; jshli@lzu.edu.cn
†Xinyu Chen and Jiang Wang contributed equally to this work.
[1]National and Local Joint Engineering Laboratory for Optical Conversion Materials and Technology, Key Laboratory of Special Function Materials and Structure Design of the Ministry of Education, and School of Physical Science and Technology, Lanzhou University, 222 South Tianshui Road, Lanzhou 730000, China
Full list of author information is available at the end of the article

combination of different light management modes is necessary for full spectral absorption enhancement. Meanwhile, considering the concerns related to fabrication issues, e.g., high reproducibility at low cost, simple structure for light absorbers is required.

To realize more efficient light confinement with limited effective thickness for semiconductor NW arrays, top modification using hemiellipsoid and inverted hemiellipsoid structures is introduced and systematically investigated on the light management behaviors in this paper. Owing to the synergetic effect of effective antireflection and light scattering, light confinement is significantly boosted with reduced effective thickness as compared to the NW arrays without modification. For the case of GaAs NW arrays, 90% and 95% of the incident photons with the energy larger than the bandgap energy can be trapped by the inverted hemiellipsoid-modified NW arrays with the effective thickness of ~ 180 and 270 nm. Moreover, further study indicates that the related structures deliver excellent light confinement under oblique incidence.

Methods

In this study, squarely arranged NW arrays (see Fig. 1a) with an optimized period of 600 nm [56, 62] are investigated under different structural parameters of the nanowire diameter (D), total height (H), and modification height (h), as labeled in Fig. 1b. To calculate the Maxwell's equations and thus the energy flux distribution of the optical systems, a finite difference time domain method is employed. Periodic boundary conditions are applied onto the side walls of a unit to construct the related arrays, and meanwhile benefit saving of the calculation source and time. At the upper and bottom bounds of the unit, the perfect matching layer boundary is used to absorb all outgoing photons and thus to determine light reflection (R) and transmission (T). Then light absorption (A) is obtained following the relationship of $A = 1–R–T$.

In this paper, the representative semiconductor optoelectronic material, GaAs, is adopted for investigation. Considering the bandgap energy of 1.42 eV and the main energy region of the solar irradiation, optical behaviors in a spectral range of 300–1000 nm are investigated. To more quantitatively compare light trapping of the optical systems, normalized theoretical photocurrent density, ${}^{N}J_{ph}$, is adopted [27, 63], which is defined as the ratio of the theoretical photocurrent density of the investigated structure to that (~ 32.0 mA/cm^2 at AM 1.5G [64] illumination for GaAs) of an ideal absorber with the same bandgap energy both at an internal quantum efficiency of 100%.

Results and Discussion

Figure 2 summarizes ${}^{N}J_{ph}$ as a function of h for the hemiellopsoid- and inverted hemiellipsoid-modified GaAs NW arrays with H of (a) 1000, (b) 2000, and (c) 3000 nm; and D of 100, 300 and 500 nm. One notes that ${}^{N}J_{ph}$ for all arrays with D of 100 nm monotonously decreases with the increased h. However, for such arrays with larger D of 300 and 500 nm, enhanced light confinement can be generally observed after introducing top modification with appropriate sizes, except for the case of $D = 300$ nm and $H = 1000$ nm. Moreover, the thicker the NWs, the more remarkable enhancement of light confinement can be realized. It is notable that, as exhibited in Fig. 2a, ${}^{N}J_{ph}$ of 0.90 and 0.95 can be achieved for the inverted hemiellipsoid modification with the effective

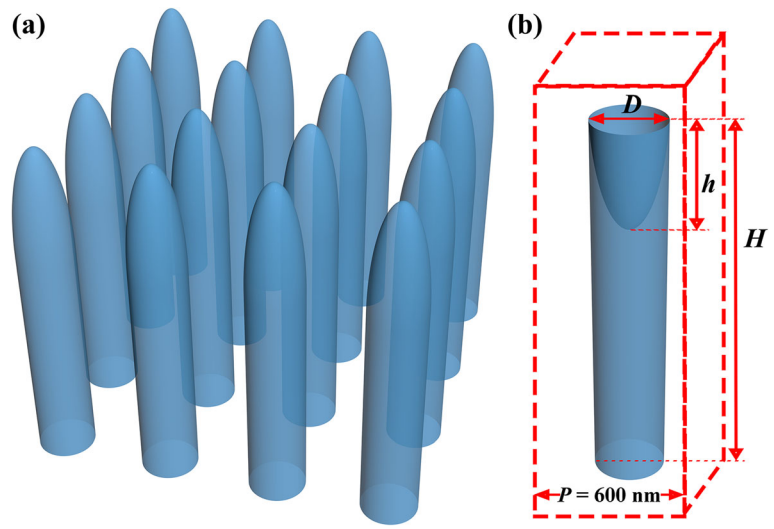

Fig. 1 **a** Schematic of a hemiellipsoid-modified NW array, and **b** a unit of an inverted hemiellipsoid-modified NW array for optical simulations. The structural parameters investigated in this study are the nanowire diameter (D), total height (H), and modification height (h) as labeled

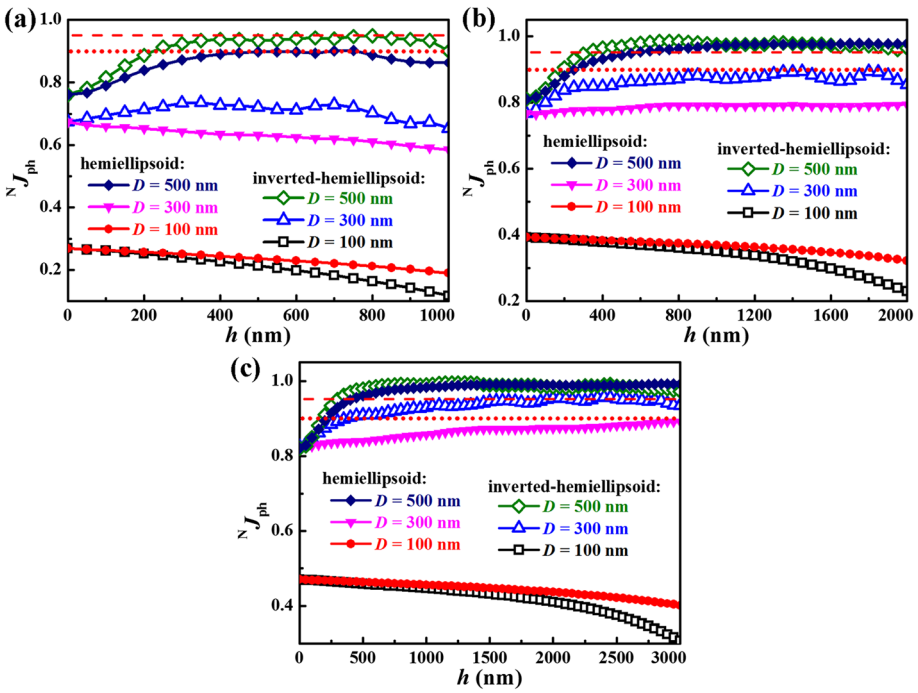

Fig. 2 Normalized theoretical photocurrent density ($^{N}J_{ph}$) for the hemiellipsoid- and inverted hemiellipsoid-modified GaAs NW arrays as a function of the hemiellipsoid height (h) at different total heights of **a** 1000, **b** 2000, and **c** 3000 nm. The wire diameters (D) are 100, 300 and 500 nm. The red dot line and red dash line in each figure denote the values of $^{N}J_{ph}$ of 0.90 and 0.95, respectively

thicknesses of only ~ 180 and 270 nm for the array with D = 500 nm, $H = h$ = 1000 nm and the array with D = 500 nm, H = 1000 nm and h = 750 nm, respectively.

It is well known that antireflection is an inherent function for NW arrays due to the reduced difference between refractive indices of the surrounding environment (normally air) and optical structure as compared to their flat wafer/film counterparts [27, 52]. However, antireflection does not consequently result in effective light absorption because of the possible enhancement of light transmission through the absorbers. In this study, the arrays with D of 100 nm possess the lowest filling ratio and thus the smallest effective refractive index. Although these arrays exhibit excellent antireflection, light transmission is significantly strong, especially in the long wavelength regime (see Fig. 3a), i.e., the high-density region of photons. Furthermore, as indicated in Fig. 3a, top modification has little contribution to antireflection, but leads to enhanced light transmission, thus making light absorption worse (see Fig. 3b), and resulting in the decrease of $^{N}J_{ph}$ for the 100 nm NW diameter arrays. In addition, one notes that the main light confinement mechanism is the HE_{11} leaky mode (see the inset of Fig. 3b) for the NW arrays of D = 100 nm [65].

For the NW arrays with larger D of 300 and 500 nm, the filling ratio and thus the effective refractive index increase, and light reflection becomes evident, as shown in Fig. 3c. For these arrays, appropriate modification using both hemiellipsoid and inverted hemiellipsoid can remarkably reduce light reflection, thus enhances light absorption (see Fig. 3c and e). Moreover, it is evident that excellent light confinement can be achieved in a broad range of modification height, thus providing convenience for fabricating the related high-performance devices. For example, as exhibited in Fig. 2b, $^{N}J_{ph}$ of 0.95 can be achieved for a 500 nm diameter NW array with inverted hemiellipsoid in range of 350–2000 nm or with hemiellipsoid in range of 600–2000 nm. However, excessive modification (i.e., h is too large) especially for the case using inverted hemiellipsoids would lead to significantly enhanced light transmission and reduced light absorption around the bandgap energy, as exhibited in Fig. 3d and e. Accordingly, the first increase and following decrease of $^{N}J_{ph}$ is observed for the related NW arrays (see Fig. 2).

Figure 3f shows the absorption spectra of the pure NW arrays with D of 100, 300 and 500 nm, and H of 2000 nm. It is evident that light absorption edge shifts towards long wavelength, and meanwhile the main light management mechanism changes from leaky mode to light scattering as D increases. Moreover, for NWs with D of 500 nm, some absorption oscillations around 800 nm can be observed, which are attributed to the guided longitudinal resonances, as exhibited in the inset of Fig. 3f. It is known that as D increases, the threshold/

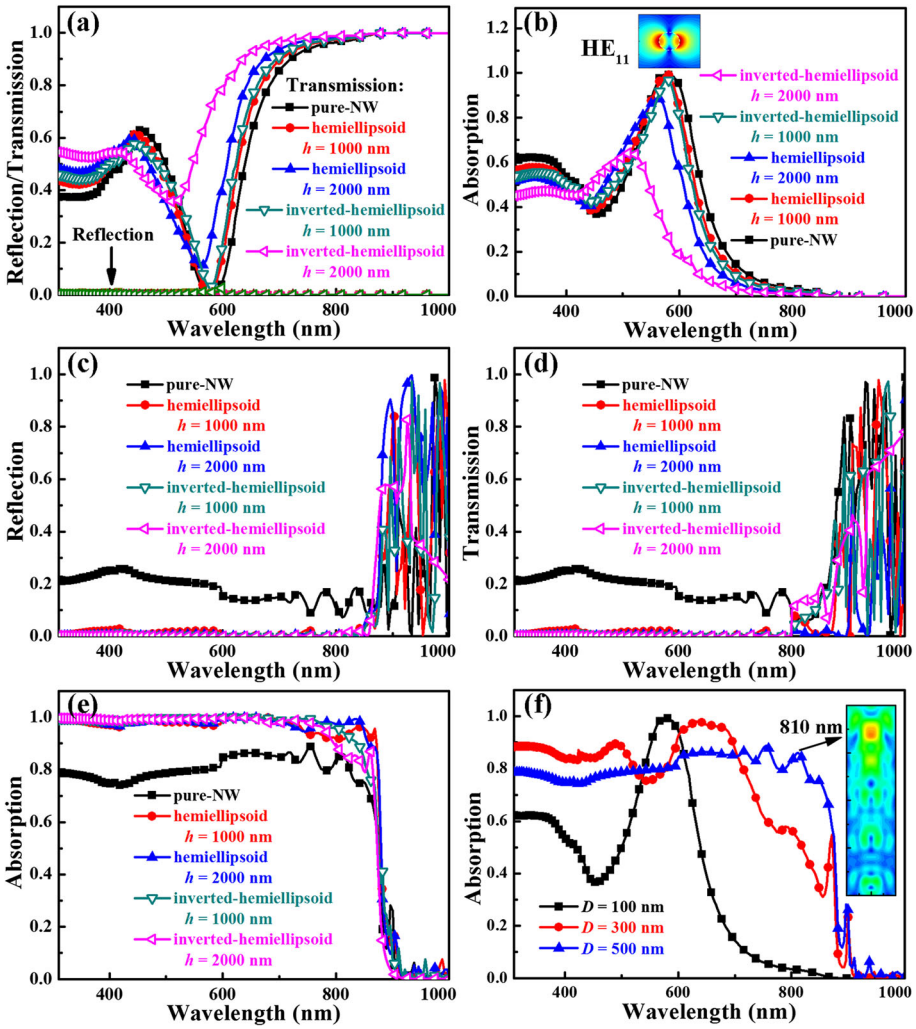

Fig. 3 **a** Reflection/transmission and **b** absorption of the arrays of $H = 2000$ nm and $D = 100$ nm. **c** Reflection, **d** transmission, and **e** absorption of the arrays of $H = 2000$ nm and $D = 500$ nm. **f** Absorption of the pure NW arrays with D of 100, 300, and 500 nm and $H = 2000$ nm. The inset of **b** shows the electric field strength distribution of the HE_{11} mode, and the white dotted circle outlines the wire periphery. The inset of **f** exhibits the electric field strength distribution of the pure NW array with $H = 2000$ nm and $D = 500$ nm at the wavelength of 810 nm

longest wavelength that can form a guided longitudinal mode also increases [56, 57]. For long-wavelength light, the amplitude decay when propagating along the wire axis is relatively weaker than that of short-wavelength light because of the smaller absorption coefficient. If the wire length is not too long, the reflected wave from the NW bottom can interfere with the incoming wave to form the guided longitudinal resonances.

To further understand influence of top modification on light management, spatial distribution of the carrier generation rate for the arrays ($H = 2000$ nm and $D = 500$ nm) modified by hemiellipsoids ($h = 500$ nm) and inverted hemielliopsoids ($h = 500$ nm) at AM 1.5G illumination is shown in Fig. 4. The corresponding distribution in the pure NW array with H and D of 2000 and 500 nm is also presented for comparison. It is obvious that the distribution region of photo-generated carriers is expanded owing to the synergetic effect of enhanced antireflection and light scattering after introducing the appropriate top modification. It is consistent with the boosted ${}^{N}J_{ph}$/enhanced light confinement for the modified arrays, as exhibited in Fig. 2b. Moreover, the expansion of the photo-generated carrier distribution is beneficial for carrier collection especially for the planar *pn* junction configuration, and meanwhile makes the structures more tolerable to bulk defects/poor material qualities. It is worth noting that compared to the pure NW array, top modification also leads to the remarkably increased carrier density on the surface, and surface passivation is necessary to reduce surface recombination losses of photo-generated carriers for such arrays [66, 67].

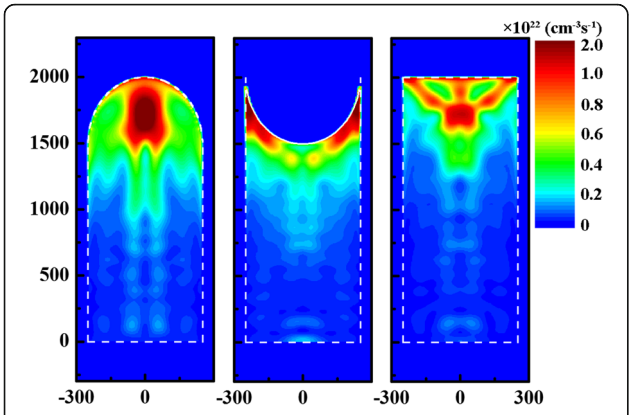

Fig. 4 Spatial distribution of the photo-generated carrier generation rate at AM 1.5G illumination for the arrays ($H = 2000$ nm and $D = 500$ nm) top-modified by (left) hemiellipsoids ($h = 500$ nm) and (middle) inverted hemiellipsoids ($h = 500$ nm). The generation rate (right) in the pure NW array of $H = 2000$ nm and $D = 500$ nm is presented for comparison

As an excellent light absorber, effective light trapping under oblique incidence is necessary. Figure 5 exhibits the absorption spectra at the incident angle, $\alpha = 0$, 30 and 60 degrees (°) for the (a) hemiellipsoid- and (b) inverted hemiellipsoid-modified GaAs NW arrays with the same structural parameters to the arrays shown in Fig. 4. It is remarkable that even at $\alpha = 60°$, only limited degradation is observable, indicating excellent omnidirectional light confinement by both modifications. The calculated photocurrent density, J_{ph} for these two arrays is summarized in the inset of Fig. 5a and b. One notes that compared to J_{ph} of ~ 27.7 and 16.0 mA/cm^2 for an ideal GaAs absorber at $\alpha = 30°$ and 60°, respectively, the corresponding value for both modified NW arrays only shows limited reduction.

It is known that for experimentally fabricated NWs, the surfaces are normally not such smooth like the ones adopted in the simulations. To check the validity of the simulation results for guiding experimental study, optical characteristics of the GaAs NW arrays with an ortho-hexagonal wire cross-section were simulated and compared with that of the corresponding NW arrays with a circle wire cross-section. Figure 6 compares the absorption spectra of these two kinds of arrays with the same volume (characterized by the diameter (100, 300 and 500 nm) of the circle NWs) and wire length of 2 μm in the spectral range of 310 nm (4 eV) to 873.2 nm (1.42 eV, i.e., the bandgap energy of GaAs). One notes that there are no evident differences of the optical behaviors between these two kinds of NW arrays in the considered spectral range. Accordingly, it is believed that the simulation results concluded from the NW arrays with a circle wire cross-section are also applicable to other arrays with a different wire cross-section.

Moreover, from the above discussion, it is evidenced that combination of the top modification for spatial modulation of the refractive index and enhanced light scattering by the bottom structure with matched characteristic dimension is an easily operated guideline for guiding design of high-performance light absorbers.

Conclusions

In this paper, top modification of semiconductor nanowires using hemiellipsoids and inverted hemiellipsoids is introduced for further improving light confinement in the corresponding arrays. Systematic investigation unveils that high performance light management at limited effective thicknesses can be realized owing to the synergetic effect of improved antireflection and light scattering after introducing appropriate modification. For example, the inverted hemiellipsoid-modified GaAs nanowire array can trap 90% and 95% of the incident photons with the energy larger than the bandgap energy at the effective thickness of only ~ 180 and 270 nm. It is found that the top-modified NW arrays exhibit excellent light trapping capability in a broad range of the

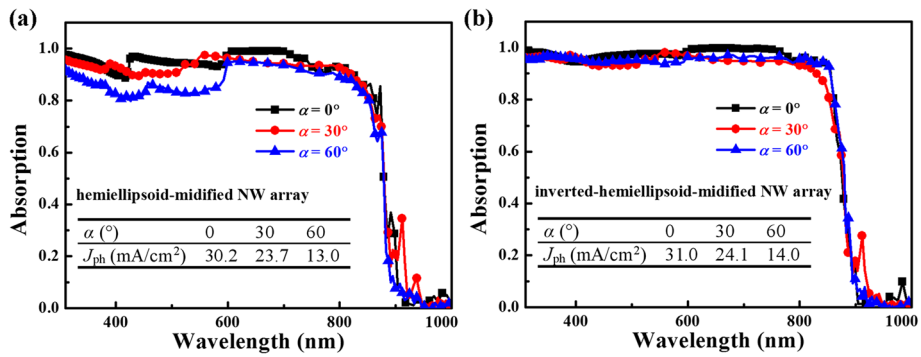

Fig. 5 Absorption spectra of the **a** hemiellipsoid- and **b** inverted hemiellipsoid-modified GaAs NW arrays ($H = 2000$ nm, $D = 500$ nm, and $h = 500$ nm) at the incident angle (α) of 0, 30, and 60°. The inset tables summarize the theoretical photocurrent density (J_{ph}) for these two top-modified NW arrays at the corresponding incident angles, respectively

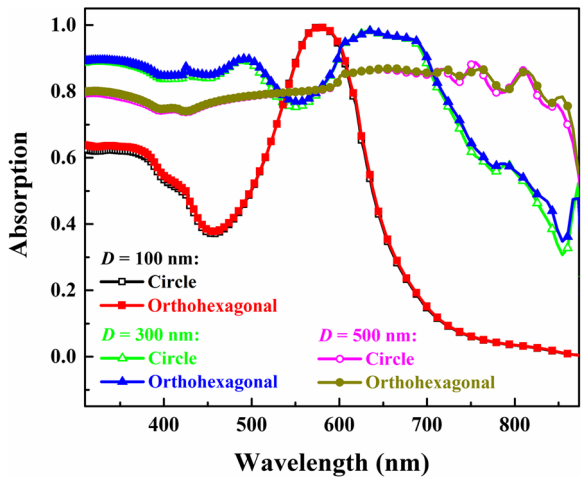

Fig. 6 Comparison of the absorption spectra of the GaAs pure NW arrays with the circle and orthohexagonal wire cross-sections. The array period and wire length are 600 nm and 2 μm, respectively. The wire volumes for the corresponding NW arrays are the same and characterized by the diameter (100, 300, and 500 nm) of the NWs with a circle cross-section

modification height. Meanwhile, spatial distribution of the photo-generated carriers is expanded for the modified nanowire arrays compared to the corresponding one without top modification, further indicating the improved light management. It would facilitate carrier collection, especially for the planar *pn* junction configuration. Moreover, further study indicates that the modified optical structures exhibit excellent omnidirectional light confinement, as expected for advanced light absorbers.

Abbreviations

J_{ph}: photocurrent density; ${}^{N}J_{ph}$: normalized theoretical photocurrent density; NW: nanowire; PV: photovoltaic

Funding

This work was supported by the National Natural Science Foundation of China (NSFC) (61376068, 11304132, 11304133, 11405144); Fundamental Research Funds for the Central Universities (Grant nos. lzujbky-2017-178 and lzujbky-2017-181).

Availability of Data and Materials

The datasets supporting the conclusions of this article are included within the article.

Authors' Contributions

XYC and JW performed the simulation work and writing of the manuscript. YLL and JSL supervised the research and revised the manuscript. PFS, QML, DQL, QC,and DYH reviewed and edited the manuscript. All authors read and approved the final manuscript.

Competing Interests

The authors declare that they have no competing interests.

Publisher's Note

Author details

[1]National and Local Joint Engineering Laboratory for Optical Conversion Materials and Technology, Key Laboratory of Special Function Materials and Structure Design of the Ministry of Education, and School of Physical Science and Technology, Lanzhou University, 222 South Tianshui Road, Lanzhou 730000, China. [2]Institute of Electromagnetics and Acoustics, Department of Electronic Science, and Fujian Provincial Key Laboratory of Plasma and Magnetic Resonance, Xiamen University, Xiamen 361005, China.

Received: 3 March 2018 Accepted: 6 August 2018
Published online: 15 August 2018

References

1. Hoffmann W (2006) PV solar electricity industry: market growth and perspective. Sol Energy Mater Sol Cells 90:3285–3311
2. Zhao DW, Sun XW, Jiang CY, Kyaw AKK, Lo GQ, Kwong DL (2008) Efficient tandem organic solar cells with an Al/MoO_3 intermediate layer. Appl Phys Lett 93:083305
3. Petermann JH, Zielke D, Schmidt J, Haase F, Rojas EG, Brendel R (2012) 19%-efficient and 43 μm-thick crystalline Si solar cell from layer transfer using porous silicon. Prog Photovolt Res Appl 20:1–5
4. Ramos FJ, Oliva-Ramírez M, Nazeeruddin MK, Graetzel M, González-Elipe AR, Ahmad S (2016) Light management: porous 1-dimensional nanocolumnar structures as effective photonic crystals for perovskite solar cells. J Mater Chem A 4:4962–4970
5. Wu S, Cui W, Aghdassi N, Song T, Duhm S, Lee ST, Sun B (2016) Nanostructured Si/organic heterojunction solar cells with high open-circuit voltage via improving junction quality. Adv Funct Mater 26:5035–5041
6. Šúri M, Huld TA, Dunlop ED, Ossenbrink HA (2007) Potential of solar electricity generation in the European Union member states and candidate countries. Sol Energy 81:1295–1305
7. Zhao Y, Han XX, Xu B, Li W, Li J, Li JJ, Wang M, Dong C, Ju P, Li JS (2017) Enhancing open-circuit voltage of solution-processed $Cu_2ZnSn(S,Se)_4$ solar cells with Ag substitution. IEEE J Photovolt 7:874–881
8. Guerrero A, Garcia-Belmonte G (2017) Recent advances to understand morphology stability of organic photovoltaics. Nano-Micro Lett. 9:10
9. Wang YZ, Shao PF, Chen Q, Li YL, Li JS, He DH (2017) Nanostructural optimization of silicon/PEDOT:PSS hybrid solar cells for performance improvement. J Phys D Appl Phys 50:175105
10. Reddy KG, Deepak TG, Anjusree GS, Thomas S, Vadukumpully S, Subramanian KRV, Nair SV, Nair AS (2014) On global energy scenario, dye-sensitized solar cells and the promise of nanotechnology. Phys Chem Chem Phys 16:6838
11. Zhong SH, Wang WJ, Zhuang YF, Huang ZG, Shen WZ (2016) All-solution-processed random Si nanopyramids for excellent light trapping in ultrathin solar cells. Adv Funct Mater 26:4768–4777
12. Lin QF, Lu LF, Tavakoli MM, Zhang C, Lui GC, Chen Z, Chen XY, Tang L, Zhang DQ, Lin YJ, Chang PC, Li DD, Fan ZY (2016) High performance thin film solar cells on plastic substrates with nanostructure-enhanced flexibility. Nano Energy 22:539–547
13. Peng KQ, Lu AJ, Zhang RQ, Lee ST (2008) Motility of metal nanoparticles in silicon and induced anisotropic silicon etching. Adv Funct Mater 18:3026–3035
14. Wang H, Wang JX, Hong L, Tan YH, Tan CS, Rusli (2016) Thin film silicon nanowire/PEDOT: PSS hybrid solar cells with surface treatment. Nanoscale Res. Lett 11(1):311
15. Goodrich A, Hacke P, Wang Q, Sopori B, Margolis R, James TL, Woodhouse M (2013) A wafer-based monocrystalline silicon photovoltaics road map: utilizing known technology improvement opportunities for further reductions in manufacturing costs. Sol Energy Mater Sol Cells 114:110–135
16. Deschler F, Price M, Pathak S, Klintberg LE, Jarausch DD, Higler R, Huttner S, Leijtens T, Stranks SD, Snaith HJ, Atature M, Phillips RT, Friend RH (2014) High photoluminescence efficiency and optically pumped lasing in solution-processed mixed halide perovskite semiconductors. J Phys Chem Lett 5:1421–1426
17. Beiley ZM, McGehee MD (2012) Modeling low cost hybrid tandem photovoltaics with the potential for efficiencies exceeding 20%. Energy Environ Sci 5:9173–9179
18. You JB, Hong ZR, Yang YM, Chen Q, Cai M, Song TB, Chen CC, Lu SR, Liu YS, Zhou HP, Yang Y (2014) Low-temperature solution-processed perovskite solar cells with high efficiency and flexibility. ACS Nano 8:1674–1680

19. Shi B, Liu BF, Luo JS, Li YL, Zheng CC, Yao X, Fan L, Liang JH, Ding Y, Wei CC, Zhang DK, Zhao Y, Zhang XD (2017) Enhanced light absorption of thin perovskite solar cells using textured substrates. Sol Energy Mater Sol Cells 168:214–220
20. Ying ZQ, Liao MD, Yang X, Han C, Li JQ, Li JS, Li YL, Gao PQ, Ye JC (2016) High-performance black multicrystalline silicon solar cells by a highly simplified metal-catalyzed chemical etching method. IEEE J. Photovolt. 6: 888–893
21. Wang KX, Yu ZF, Liu V, Cui Y, Fan SH (2012) Absorption enhancement in ultrathin crystalline silicon solar cells with antireflection and light-trapping nanocone gratings. Nano Lett 12:1616–1619
22. Li JS, Yu HY, Wong SM, Zhang G, Lo GQ, Kwong DL (2009) Surface nanostructure optimization for solar energy harvesting in Si thin film based solar cells. IEEE Technical Digest-Int Electron Devices Meeting:511
23. Mendes MJ, Araújo A, Vicente A, Águas H, Ferreira I, Fortunato E, Martins R (2016) Design of optimized wave-optical spheroidal nanostructures for photonic-enhanced solar cells. Nano Energy 26:286–296
24. Svensson J, Chen Y, Anttu N, Pistol ME, Wernersson LE (2017) Increased absorption in InAsSb nanowire clusters through coupled optical modes. Appl Phys Lett 110:081104
25. Zhou SQ, Yang ZH, Gao PQ, Li XF, Yang X, Wang D, He J, Ying ZQ, Ye JC (2016) Wafer-scale integration of inverted nanopyramid arrays for advanced light trapping in crystalline silicon thin film solar cells. Nanoscale Res Lett 11:194
26. Li XC, Li JS, Chen T, Tay BK, Wang JX, Yu HY (2010) Periodically aligned Si nanopillar arrays as efficient antireflection layers for solar cell applications. Nanoscale Res Lett 5:1721–1726
27. Chen XY, Wang J, Qin SC, Chen Q, Li YL, Li JS, He DY (2017) Wedge-shaped semiconductor nanowall arrays with excellent light management. Opt Lett 42:3928–3931
28. Fan ZY, Kapadia R, Leu PW, Zhang XB, Chueh YL, Takei K, Yu K, Jamshidi A, Rathore AA, Ruebusch DJ, Wu M, Javey A (2010) Ordered arrays of dual-diameter nanopillars for maximized optical absorption. Nano Lett 10: 3823–3827
29. Li YL, Chen Q, He DY, Li JS (2014) Radial junction Si micro/nano-wire array photovoltaics: recent progress from theoretical investigation to experimental realization. Nano Energy 7:10–24
30. Wong SM, Yu HY, Li JS, Li YL, Singh N, Lo PGQ, Kwong DL (2011) Si nanopillar array surface-textured thin-film solar cell with radial p-n junction. IEEE Electron Device Lett 32:176–178
31. Elbersen R, Vijselaar W, Tiggelaar RM, Gardeniers H, Huskens J (2016) Effects of pillar height and junction depth on the performance of radially doped silicon pillar arrays for solar energy applications. Adv Energy Mater 6: 1501728
32. Wang YM, Chen Y, Zhao WQ, Ding LW, Wen L, Li HX, Jiang F, Su J, Li LY, Liu NH, Gao YH (2017) A self-powered fast-response ultraviolet detector of p-n homojunction assembled from two ZnO-based nanowires. Nano-Micro Lett 9:11
33. Wong SM, Yu HY, Li YL, Li JS, Sun XW, Singh N, Lo PGQ, Kwong DL (2011) Boosting short-circuit current with rationally designed periodic Si nanopillar surface texturing for solar cells. IEEE Tran Electron Dev 58:3224–3229
34. Tian BZ, Zheng XL, Kempa TJ, Fang Y, Yu NF, Yu GH, Huang JL, Lieber CM (2007) Coaxial silicon nanowires as solar cells and nanoelectronic power sources. Nature 449:885–889
35. McAlpine MC, Ahmad H, Wang DW, Heath JR (2007) Highly ordered nanowire arrays on plastic substrates for ultrasensitive flexible chemical sensors. Nat Mater 6:379–384
36. Wang XX, Yang ZH, Gao PQ, Yang X, Zhou SQ, Wang D, Liao MD, Liu PP, Liu ZL, Wu SD, Ye JC, Yu TB (2017) Improved optical absorption in visible wavelength range for silicon solar cells via texturing with nanopyramid arrays. Opt Express 25:10464–10472
37. Huang NF, Lin CX, Povinelli ML (2012) Broadband absorption of semiconductor nanowire arrays for photovoltaic applications. J Opt 14:981–986
38. Li JS, Yu HY, Wong SM, Li XC, Zhang G, Lo PGQ, Kwong DL (2009) Design guidelines of periodic Si nanowire arrays for solar cell application. Appl Phys Lett 95:243113
39. Li JS, Yu HY, Wong SM, Zhang G, Sun XW, Lo PGQ, Kwong DL (2009) Si nanopillar array optimization on Si thin films for solar energy harvesting. Appl Phys Lett 95:033102
40. Adachi MM, Anantram MP, Karim KS (2013) Core-shell silicon nanowire solar cells. Sci Rep 3:1546
41. Lee E, Zhou K, Gwon M, Jung JY, Lee JH, Kim DW (2013) Beneficial roles of Al back reflectors in optical absorption of Si nanowire array solar cells. J. Appl. Phys 114:093516
42. Cao LY, Fan PY, Vasudev AP, White JS, Yu ZF, Cai WS, Schuller JA, Fan SH, Brongersma ML (2010) Semiconductor nanowire optical antenna solar absorbers. Nano Lett 10:439–445
43. Yang ZH, Li XF, Lei DY, Shang AX, Wu SL (2015) Omnidirectional absorption enhancement of symmetry-broken crescent-deformed single-nanowire photovoltaic cells. Nano Energy 13:9–17
44. Michallon J, Bucci D, Morand A, Zanuccoli M, Consonni V, Kaminski-Cachopo A (2014) Light trapping in ZnO nanowire arrays covered with an absorbing shell for solar cells. Opt Express 22:A1174–A1189
45. Li YH, Yan X, Wu Y, Zhang X, Ren XM (2015) Plasmon-enhanced light absorption in GaAs nanowire array solar cells. Nanoscale Res Lett 10:436
46. Jeong S, McGehee MD, Cui Y (2013) All-back-contact ultra-thin silicon nanocone solar cells with 13.7% power conversion efficiency. Nat. Commun 4:2950
47. Wang H, Wang JX, Rusli (2015) Hybrid Si nanocones/PEDOT:PSS solar cell. Nanoscale Res Lett 10:191
48. Jeong S, Garnett EC, Wang S, Yu ZF, Fan SH, Brongersma ML, McGehee MD, Cui Y (2012) Hybrid silicon nanocone-polymer solar cells. Nano Lett 12: 2971–2976
49. Li JS, Yu HY, Wong SM, Zhang G, Lo GQ, Kwong DL (2010) Si nanocone array optimization on crystalline Si thin films for solar energy harvesting. J Phys D Appl Phys 43:255101
50. Wang BM, Leu PW (2012) Enhanced absorption in silicon nanocone arrays for photovoltaics. Nanotechnology 23:194003
51. Baek WH, Seo I, Yoon TS, Lee HH, Yun CM, Kim YS (2009) Hybrid inverted bulk heterojunction solar cells with nanoimprinted TiO_2 nanopores. Sol Energy Mater Sol Cells 93:1587–1591
52. Li JS, Yu HY, Li YL, Wang F, Yang MF, Wong SM (2011) Low aspect-ratio hemispherical nanopit surface texturing for enhancing light absorption in crystalline Si thin film-based solar cells. Appl Phys Lett 98:021905
53. Gao PQ, Wang HZ, Sun ZX, Han WQ, Li JS, Ye JC (2013) Efficient light trapping in low aspect-ratio honeycomb nanobowl surface texturing for crystalline silicon solar cell applications. Appl Phys Lett 103:253105
54. Gao TC, Stevens E, Lee JK, Leu PW (2014) Designing metal hemispheres on silicon ultrathin film solar cells for plasmonic light trapping. Opt Lett 39: 4647–4650
55. Li YL, Yu HY, Li JS, Wong SM, Sun XW, Li XL, Cheng CW, Fan HJ, Wang J, Singh N, Lo PGQ, Kwong DL (2011) Novel silicon nanohemisphere-array solar cells with enhanced performance. Small 7:3138–3143
56. Li YL, Gao PQ, Chen Q, Yang JM, Li JS, He DY (2016) Nanostructured semiconductor solar absorbers with near 100% absorption and related light management picture. J Phys D Appl Phys 49:215104
57. Wang BM, Leu PW (2012) Tunable and selective resonant absorption in vertical nanowires. Opt Lett 37:3756–3758
58. Eisenlohr J, Tucher N, Hauser H, Graf M, Benick J, Bläsi B, Goldschmidt JC, Hermle M (2016) Efficiency increase of crystalline silicon solar cells with nanoimprinted rear side gratings for enhanced light trapping. Sol Energy Mater Sol Cells 155:288–293
59. Cao LY, White JS, Park JS, Schuller JA, Clemens BM, Brongersma ML (2009) Engineering light absorption in semiconductor nanowire devices. Nat Mater 8:643–647
60. Shao PF, Chen XY, Guo X, Zhang WJ, Chang FZ, Liu QM, Chen Q, Li JS, Li YL, He DY (2017) Facile embedding of SiO_2 nanoparticles in organic solar cells for performance improvement. Org Electron 50:77–81
61. Jing C, Rawson FJ, Zhou H, Shi X, Li WH, Li DW, Long YT (2014) New insights into electrocatalysis based on plasmon resonance for the real-time monitoring of catalytic events on single gold nanorods. Anal Chem 86: 5513–5518
62. Li JS, Yu HY, Li YL (2012) Solar energy harnessing in hexagonally arranged Si nanowire arrays and effects of array symmetry on optical characteristics. Nanotechnology 23:194010
63. Raja W, Schmid M, Toma A, Wang H, Alabastri A, Zaccaria RP (2017) Perovskite nanopillar array based tandem solar cell. ACS Photonics 4:2025–2035
64. ASTM, Reference Solar Spectral Irradiance: Air Mass 1.5 https://www.nrel.gov/grid/solar-resource/spectra-am1.5.html. Accessed 3 March 2018
65. Wen L, Li XH, Zhao ZF, Bu SJ, Zeng XS, Huang JH, Wang YQ (2012) Theoretical consideration of III-V nanowire/Si triple-junction solar cells. Nanotechnology 23:505202

66. Li Z, Wenas YC, Fu L, Mokkapati S, Tan HH, Jagadish C (2015) Influence of electrical design on core–shell GaAs nanowire array solar cells. IEEE J. Photovolt. 5:854–864
67. Mallorquí AD, Alarcón-Lladó E, Mundet IC, Kiani A, Demaurex B, Wolf SD, Menzel A, Zacharias M, i Morral AF (2014) Field-effect passivation on silicon nanowire solar cells. Nano Res 8:673–681